# Ferrite Coating on Iron Particles in Aqueous Solution: Effect of Surface Functionalization

Guicheteau R[1], Bobet JL[1], Lu YF[2], Troedec ML[1] and Silvain JF[1,2*]

[1]CNRS-Université de Bordeaux, ICMCB, 87 Avenue du Dr Schweitzer, 33608 Pessac Cedex, France
[2]Department of Electrical and Computer Engineering, University of Nebraska-Lincoln, Lincoln, NE 68588-0511 USA

## Abstract

Ferrite coating of acid treated iron particles with have been optimized using electroless process. The effect of the functionalization was monitored by XPS and SEM analysis whereas adhesion behavior of ferrite thin films was characterized using a non-conventional ultrasonic test. It is shown that acidic treatments increase the amount of hydroxyl groups on the surface of iron particles, allowing the creation of chemical bonds between the iron core and its ferrite shell. It leads to an increase of the adhesion between both materials. It is shown that the reactivity of iron particles improves the ferrite deposition process. A homogeneous adhesive ferrite coating of around 2 µm with a deposition process of 90 min has been obtained.

**Keywords:** Iron particles; NiZn ferrite; Surface treatment; Adhesion

## Introduction

With the growth of miniaturization requirement for application such as transformers, computers, and inductors or motors, soft magnetic composites (SMC) with high flux density, high permeability and low magnetic loss are under development [1-5]. These powders are composed of an iron (or its alloys) core coated with a thin electrically insulating layer. This insulating layer is generally made of a polymer [6,7] or oxides [8-10]. In these cases, as the insulating layer is a non-magnetic material, it leads to a decrease of the magnetic permeability or of the magnetic induction. One way to avoid or to reduce these properties decrease is to replace the non-magnetic layer by a magnetic electrically insulating layer. NiZn ferrite can appear as a good candidate. Abe have developed a process to deposit NiZn ferrite onto particles by an aqueous route using metal salt [11]. They reported that 1) the ferrite coating occurs thanks to the presence of hydroxyl groups (-OH) on the surface of the substrate and 2) the increase of the –OH group concentration on the surface of particles, after acid treatment, leads to an increase of the substrate reactivity. In this work, Abe et al. apparatus and process have been simplified and optimized and the effect of chemical surface treatments, of Fe particles, followed using X-ray photoelectron spectroscopy (XPS) analysis. This study demonstrates that surface reactivity of Fe particles on NiZn ferrite coating, using electroless process, is strongly link with OH groups chemically linked on Fe particles. Five different acid treatments have been tested onto Fe particles and the evolution of the XPS C1s and O1s followed. Finally the morphology and the adhesion strength of the NiZn ferrite coating, electroless deposited onto acid treated Fe particles, have been analyzed and correlated with the experimental procedures.

## Experimental

### Material

Goodfellow supplied the iron powder with an average particle size of 60 µm and purity above 99%. Metallic salt, $FeCl_2$, $4H_2O$ (98%), $NiCl_2$, $6H_2O$ (99.3%) and $ZnCl_2$ (98%), were supplied by Alfa Aesar.

### Surface functionalization

Prior to deposition, iron powders were treated by acidic solution. 20 g of iron particles were introduced into 150 ml of an acidic solution and put into an ultrasonic bath during 15 minutes.

Different acidic treatments were used:

-- Hydrochloric acid (0.2 M)

-- Nitric acid (0.2 M)

-- Citric acid (2 M)

-- Hydrochloric acid (0.2 M) then citric acid (2 M)

-- Nitric acid (0.2 M) then citric acid (2 M)

The functionalized particles were then washed 4 times with distilled water.

### Preparation of Ni-Zn ferrite insulated powder via electroless process

The wet functionalized particles were directly introduced into 150 ml of distilled water heated at 65°C (named solution 1). Then, iron chloride, nickel chloride and zinc chloride were mixed with solution 1 with concentration of 0.25 M, 0.0625 M and 0.625 M (these 3 concentrations are the optimized ones). A 200 ml aqueous solution containing KOH (0.1 M) and $NaNO_3$ (6.10-2 M) (named solution 2) were added to solution 1 at a rate of 2.5 mL/min. The rate addition has been optimized to keep the pH of the solution close to 6. The solution 1 was then stirred by mechanical agitator in open air and maintained at 65°C until the reaction was finished (i.e. after 90 min). The Fe-ferrite particles were then rinsed 4 times with distilled water and dried for 60 min at 80°C.

### Characterization

The Ni-Zn ferrite insulating layer have been characterized

using scanning electron microscopy (SEM) (TESCAN VEGA 3 SB microscope) and by X-Ray diffraction (XRD) (Philips PANalytical X'Pert PW1820 diffractometer with Cu Kα1 radiation). For XPS analysis, ThermoFisher Scientific K-ALPHA spectrometer was used with a monochromatized Al Kα source (hν = 1486.6 eV) and 200 μm spot size. A pressure of 10-7 Pa was reached in the chamber when transferring the samples. The full spectra (0-1100 eV) were obtained with constant pass energy of 200 eV and high-resolution spectra at constant pass energy of 40 eV. Charge neutralization was applied during analysis. High-resolution spectra were fitted and quantified using the CASAXPS software (Scofield sensitivity factors used for quantification).

In order to characterize the adhesion strength between the NiZn ferrite layers and the acid treated and non-treated Fe particles, a non-conventional global adhesion test has been optimized. For this test, the coated Fe particles were dispersed into a solvent (distilled water) and controlled ultrasound (power and time) was applied through a 13 mm horn. After ultrasound test, the presence of the NiZn ferrite coating on the surface of the Fe particles is analyzed using SEM. Power and duration of the ultrasound test have been previously optimized in order to obtained observable and noticeable difference. Even if no real values, of the adhesion strength can be calculated through this test, the adhesion strength of our different NiZn ferrite-Fe materials can be classified: larger one when the coating is still present onto the Fe particles after the ultrasound test and lower one when the coating has been completely removed by the ultrasound.

## Results and discussion

### Surface analysis

The aim of this study was to control the chemistry of the Fe particle surface by using a chemical treatment and to measure, after the grow of NiZn thin films onto Fe, the interfacial strength between the Fe particles and the NiZn ferrite coating. The surface chemistry of the iron particle was analyzed by XPS. The full spectra presented in Figure 1 (bold curve), shows that the surface of iron particles, before acidic treatment, was composed of iron, oxygen, carbon and manganese. The presence of 1) oxygen was due to the natural oxidation and surface contamination of iron, 2) carbon was mainly link with surface contamination and 3) manganese results from the preparation of the iron particles by suppliers. After acidic treatment (Figure 1 bright curve), no change can be highlighted. No nitrogen or chlorine species were detected meaning that the acids were sufficiently diluted to avoid nitriding or chlorination. Nevertheless, the acidic treatments tend to remove the manganese impurities present on the surface of the Fe powders. Table 1 shows the evolution of the chemistry of the near surface of the iron particles for the non-treated and the acid treated Fe particles analysed by XPS. Several points can be highlight from this table:
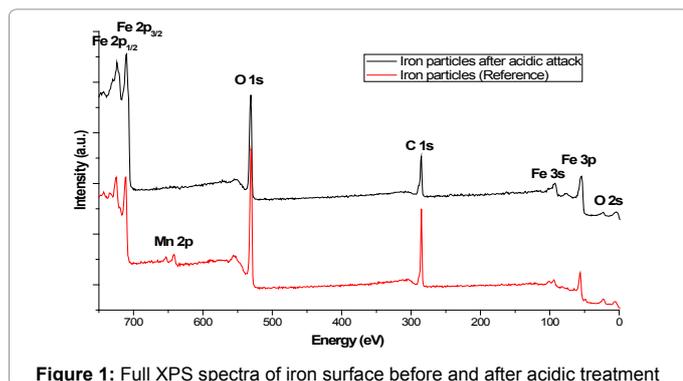


**Figure 1:** Full XPS spectra of iron surface before and after acidic treatment

| Element | Fe | Fe + 20s IB | Fe (HCl) + 20s IB | Fe (HNO₃) + 20s IB | Fe (C₆H₈O₇) + 20s IB |
|---------|-----|-------------|-------------------|--------------------|-----------------------|
| C1s | 47 | 27 | 30 | 29 | 44 |
| O1s | 44 | 53 | 48 | 35 | 28 |
| Fe2p3 | 8 | 18 | 22 | 36 | 28 |
| Mn2p3 | 1 | 2 | 0 | 0 | 0 |

**Table 1:** Evolution of the atomic concentration of the top surface of the non-treated Fe particles (before and after ion bombardment (IB) (20 s)) and of the acid treated Fe particles after 20 s of IB
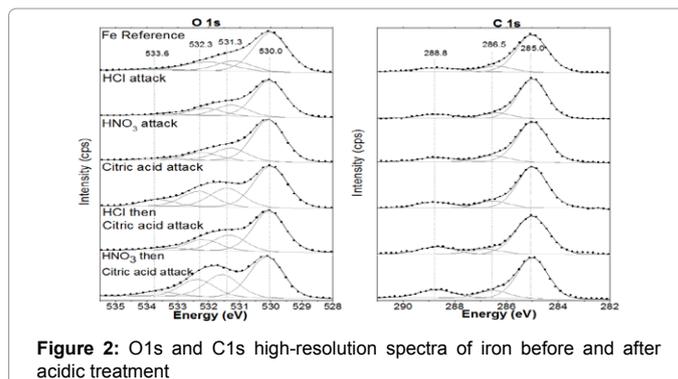


**Figure 2:** O1s and C1s high-resolution spectra of iron before and after acidic treatment

-- For the non-treated Fe particles, 20 s of ion bombardment (IB), inside the analysis chamber, tend to remove the atmosphere induced surface contamination of the particles (decrease of the C and 0 content) but have no specific effect on their surface oxidation (oxygen concentration close to 50%) and on the carbon contamination induce by the fabrication process (carbon concentration close to 30%).

-- For the acid treated Fe particles, the carbon concentration is mainly constant (close to 30%),, whatever the oxide used except for the acid citric treatment that leads to a significant increase of the carbon content (+ 15%) due to the composition of the acid ($C_6H_8O_7$) (the other acids do not contain carbon species).

-- For the treated Fe particles, the oxygen content are strongly linked with the type of oxide used and is measure to range between 22% to 36%. Choice of acid is therefore shown to be crucial if we want to optimize the oxygen concentration onto the Fe particles after treatment.

-- The presence of Mn impurity on the Fe surface completely disappear, after acid treatment, whatever the acid used.

High-resolution O 1s and C 1s spectra were deconvoluted to determine the presence of oxide/hydroxide species (Figure 2). Peak shifts due to any apparent charging were normalized with the C1s peak set to 285 eV. On the calculated spectra presented in Figure 2, the dots correspond to the experimental data, the gray curves correspond to the fitted peaks and the black curve correspond to the fitted spectrum. Four peaks were deconvoluted on the O 1s spectra at 530.0 eV, 531.3 eV, 532.3 eV and 533.6 eV, and three peaks on the C 1s spectra at 285.0 eV, 285.6 eV and 288.8 eV. According to [12] and [13], these peaks can be associated to the following bonds:

- 530.0 ± 0.1 eV can be associated to O-O bond from FeO, $Fe_2O_3$, $Fe_3O_4$, FeOOH

- 531.3 ± 0.1 eV can be associated to –OH- bond from $Fe(OH)_2$, $Fe(OH)_2$ or FeOOH

Due to the presence of carbon, it can also be associated to C=O or C-OH bonding.

| Bond | Bond Energy (eV) | Fe reference | HCl treatment | HNO$_3$ treatment | C$_6$H$_8$O$_7$ acid treatment | HCl and C$_6$H$_8$O$_7$ acid treatment | HNO$_3$ and C$_6$H$_8$O$_7$ acid treatment |
|---|---|---|---|---|---|---|---|
| **C 1s : C-C ; C-H** | 285.0 | 26 | 25 | 24 | 35 | 24 | 27 |
| **C 1s : C-O, C-OH** | 286.5 | 4 | 3 | 3 | 6 | 3 | 5 |
| **C 1s : C=O** | 288.8 | 4 | 3 | 3 | 6 | 5 | 6 |
| **Fe 2p** | 710-720 | 13 | 18 | 17 | 22 | 20 | 16 |
| **O 1s : O-O** | 530.0 | 31 | 33 | 34 | 16 | 27 | 23 |
| **O 1s : O-H or C=O** | 531.5 | 8 | 10 | 11 | 8 | 11 | 12 |
| **O 1s : (-OH)$_{ad}$, C-OH, C=O, O-CO** | 532.3 | 11 | 6 | 6 | 6 | 8 | 9 |
| **O 1s : (H$_2$O)$_{ad}$, C-OH, C=O, C-O-C** | 533.6 | 2 | 2 | 2 | 2 | 2 | 2 |
| **Mn 2p** | 640-655 | 1 | 0 | 0 | 0 | 0 | 0 |

**Table 2:** Chemical environments, bond energies (eV), and quantification (%) of the C1s and O1s species analyzed by XPS onto the treatment and non-treated Fe particles

| Treatment | No treatment | HCl | HNO$_3$ | C$_6$H$_8$O$_7$ |
|---|---|---|---|---|
| Oxide thickness (nm) | 50 | 200 | >200 | 30 |

**Table 3:** Oxide layer thickness measured by XPS



**Figure 3:** Cross-sectional SEM micrograph (BSE) of iron-ferrite composite particles before ultrasound treatment (a) and after ultrasound treatment on: non-functionalized particles (b), Fe particles after HCl treatment (c), Fe particles after HNO$_3$ treatment (d) and Fe particles after C$_6$H$_8$O$_7$ acid treatment (e)

- 532.2 ± 0.1 eV can be associated to adsorb OH. Due to the presence of carbon, it can also be associated to C-OH, C=O or O-C-O bonding.

- 533.3 ± 0.1 eV can be associated to adsorb H$_2$O. Due to the presence of carbon, it can also be associated to C-OH, C=O or O-C-O bonding.

- 283.0 ± 0.1 eV correspond to a carbon in sp3 hybridization: C-C or C-H bonding.

- 286.5 ± 0.1 eV is associated to C-O- bonding.

- 288.8 ± 0.1 eV correspond to a carbon in sp2 hybridization: C=O.

Approximate quantifications determined from these fitted spectra were obtained using Scofield sensitivity factors and are summarized in Table 2. High-resolution spectra of O 1s show an increase of O-H bond on the surface of irons particles after treatment with HCl (from 8 to 10%) and HNO$_3$ (from 8 to 11%). Almost the same behavior was observed when the particles were first treated with HCl or HNO$_3$ followed citric acid treatment (going from 8 to 11 and 12% respectively).

For the 532.3 eV peak, the relative percentage goes from 6 (for HCl and HNO3 treatment) to 8 and 9 (for HCl and HNO$_3$ treatment followed by citric acid treatment). Such increase was attributed to C-OH bond as the citric acid treatment leads to a huge increase of the relative percentage of the C-C and C-H bonds (e.g. about 25% whatever the acid to 35 for citric acid at 285 eV). This is in good agreement with the chemical composition of citric acid (C$_6$H$_8$O$_7$). The percentage of the OH species, present just after a citric acid treatment, was similar to the OH percentage analyzed on the surface of iron reference particles. However, the quantity of O-O bonding, present at 530.0 eV, and the oxygen concentration on particles surface are lower in the case of citric acid treatment (e.g. 31% for iron reference and only 16% for citric acid treatment). These measurements indicate that the oxide layer, on particles surface, was thinner after citric acid treatment. This result was confirmed by the measurement of the oxide layer (Table 3) after ion bombardment of the Fe surface followed by XPS analysis. Citric acid reduces the thickness of the oxide layer, the percentage of -OH bonds does not increase but the ratio between -OH bonds and O-O bonds have been enhanced. For nitric or hydrochloric the oxide thickness were increase (from 50 to over 200 μm).
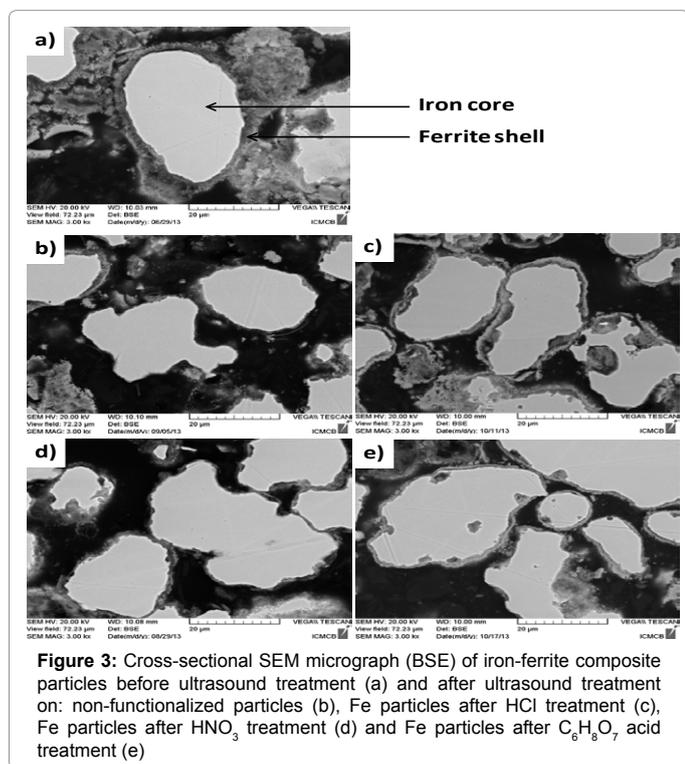
### Effect of acidic functionalization on Ferrite coating

Cross-sectional SEM micrograph of iron-ferrite core-shell particles is shown in Figure 3a. This micrograph is representative of each iron particles (with or without functionalization) after ferrite plating. The iron core is visible in white and the ferrite coating is visible, in gray, with a thickness of about 2 μm. After sonication, the ferrite coating disappeared (Figure 3b). Almost the same behavior was observed (Figure 3d) for the particles treated with nitric acid (the main part of the coating disappeared, but some traces remained present). The disappearance of the ferrite coating onto the surface of the iron particles, after sonication, should be associated with weak bonding strength between the iron surface and its coating. On the other hand, the ferrite coating is still present on Fe particles treated with chloridric acid (Figure 3c) or with citric acid (Figure 3e). On the particles functionalized with HCl and using the deposition conditions gived previously, the thickness of the ferrite coating is around 2 μm but it is less than 1 μm for the Fe particles preliminary functionalized with citric acid. Same results (Figure 3e) were obtained with the HCl or HNO$_3$ treatment followed by C$_6$H$_8$O$_7$ treatment (Figure 3).
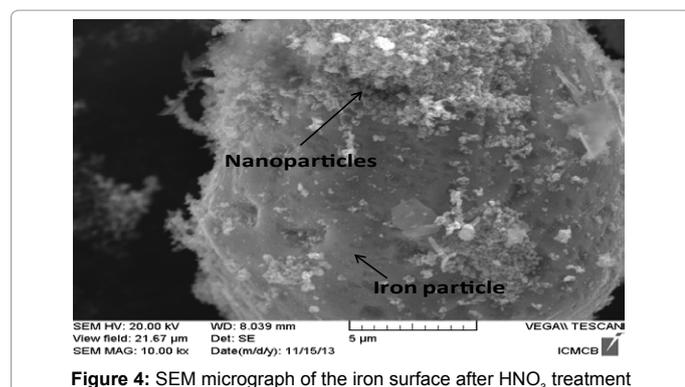
**Figure 4:** SEM micrograph of the iron surface after $HNO_3$ treatment

The functionalization of iron surface particles by acid treatment increases the amount of –OH species or increases the ratio between -OH species and O-O bonds and finally improves the adhesion strength between iron core and the ferrite coating. In the case of nitric acid treatment, a part of the ferrite coating is removed after sonication. This behavior can be explained by the presence of nanoparticles of Fe oxide on the surface of iron powder after acidic treatment (Figure 4) that should be physisorped onto the irons particles (magnetic or electrostratic) leading to weak bonds. It is also suggested that the germination and growth of the ferrite coating will occur preferentially on these nanoparticles nucleation site. Finally, the sonication treatment of the ferrite coated iron particles, which were nitric acid treated, will remove the ferrite coating which have grown onto the Fe oxide nanoparticles leading to the removal of the ferrite coating.

## Conclusion

Ni-Zn ferrite insulating layer have been grown onto iron particles using electroless process. Thickness and homogeneity of the coating were optimized through electroless process and iron surface treatment. We show that acidic treatment on iron particles allows the surface functionalization of iron with hydroxyl bonding. HCl or $HNO_3$ treatments increase the percentage of hydroxyl whereas citric acid increases -OH/O-O the ratio. It has been shown that the functionalization of iron particles increases the surface reactivity and simplifies the ferrite plating. A non-conventional global adhesion test, using controlled ultrasound apparatus, has been optimized allowing the classification of the NiZn ferrite adhesion onto iron particles. The functionalization with acidic treatments increases the adhesion between the iron core and its ferrite coating thanks to the presence of hydroxyl groups. However, this result is not confirmed in the case of nitric acid treatment. The nitric acid treatment forms magnetite nanoparticles on the iron surface. These nanoparticles had a weak interaction with iron core and were ejected after sonication, wrecking the ferrite layer.

## References

1. Bayramli E, Gölgelioglu O, Ertan HB (2005) Powder metal development for electrical motor applications. Journal of Materials Processing Technology 161: 83-88.

2. Hodgson SNB, Koniarek J, Weglinski B, Pang YX (2007) The influence of the dielectric on the properties of dielectromagnetic soft magnetic composites. investigations with silica and silica hybrid sol-gel derived model dielectric. Journal of Magnetism and Magnetic Materials 310: 83-91.

3. Shokrollahi H, Janghorban K (2007) Soft magnetic composite materials (smcs). Journal of Materials Processing Technology 189: 1-12.

4. Xiaoxin Y, Tse Zion TH, Guoyi T, Guolin S (2014) Effect of electroplastic rolling on deformability, mechanical property and microstructure evolution of Ti-6Al-4V alloy strip. Materials Characterization 98: 147-161.

5. Xiaoxin Y, Tse Zion TH, Guoyi T, Yubo G, Guolin S (2015) Influence of electropulsing globularization on the microstructure and mechanical properties of Ti-6Al-4V alloy strip with lamellar microstructure. Materials Science and Engineering: A 622: 1-6.

6. Gay DE (1997) Annealed polymer-bonded soft magnetic body. Patent US5589010.

7. Yamaguchi T, Ono T, Hoshi H, Hirakawa M, Watanabe I (1972) Process for preparing plastic coated metal powders. Patent US3935340.

8. Ochiai K, Horie H, Arima I, Morita M (1990) Compressed magnetic powder core. Patent US4919734.

9. Larker HD (1982) Method for manufacturing an object of soft-magnetic material by bonding together a mass of powder grains. Patent EP0088992.

10. Toyoda H, Mizutani R (2004) Soft magnetic material and method for producing the same. Patent US20070036669.

11. Abe M (2000) Ferrite plating: A chemical method preparing oxide magnetic films at 24-100°c, and its applications. Electrochimica Acta 45: 3337-3343.

12. Grosvenor AP, Kobe BA, McIntyre NS (2004) Studies of the oxidation of iron by air after being exposed to water vapor using angle-resolved x-ray photoelectron spectroscopy and quases. Surface and Interface Analysis 36: 1637-1641.

13. Sobol PE, Bomben KD, Moulder JF, Stickle WF (1995) Handbook of X-ray Photoelectron Spectroscopy. Physical Electronics, Inc.